SUPER-DROPLET APPROACH TO SIMULATE PRECIPITATING TRADE-WIND CUMULI
COMPARISON OF MODEL RESULTS WITH RICO AIRCRAFT OBSERVATIONS

Sylwester Arabas[1] and Shin-ichiro Shima[2,*]

1: Institute of Geophysics, Faculty of Physics, University of Warsaw, Poland
2: Graduate School of Simulation Studies, University of Hyogo, Kobe, Japan
*: Affiliation at the time of research: Japan Agency for Marine-Earth Science and Technology, Kanagawa, Japan

paper draft on arXiv

http://arxiv.org/pdf/1205.3313
comments welcome! (sarabas@igf.fuw.edu.pl)

simulation set-up

RICO composite case (van Zanten et al. 2011)
Nagoya University Cloud-Resolving Storm Simulator (CReSS, Tsuboki, 2008)

list of model runs

run label	grid	dx=dy	dz	time-steps [s]	sd density [cm^{-3}]
sdm-coarse-8	64 × 64 ×100	100m	40m	1.00/0.100/0.25/1.0/1.0	2.0×10^{-11}
sdm-coarse-32	64 × 64 ×100	100m	40m	1.00/0.100/0.25/1.0/1.0	8.0×10^{-11}
sdm-coarse-128	64 × 64 ×100	100m	40m	1.00/0.100/0.25/1.0/1.0	3.2×10^{-10}
sdm-coarse-512	64 × 64 ×100	100m	40m	1.00/0.100/0.25/1.0/1.0	1.3×10^{-09}
sdm-middle-8	128×128×200	50m	20m	0.50/0.050/0.25/1.0/1.0	1.6×10^{-10}
sdm-middle-32	128×128×200	50m	20m	0.50/0.050/0.25/1.0/1.0	6.4×10^{-10}
sdm-middle-128	128×128×200	50m	20m	0.50/0.050/0.25/1.0/1.0	2.6×10^{-09}
sdm-high-8	256×256×400	25m	10m	0.25/0.025/0.25/1.0/0.5	1.3×10^{-09}

The run label denotes which grid resolution (coarse, middle or high) and super-droplet number density was chosen. Coarse resolution corresponds to a quarter of the domain from the original RICO set-up (i.e. grid box size of 100×100×40 m with 64×64×100 grid points); the middle and high resolutions denote settings resulting in halved and quartered grid box dimensions, respectively (with the domain size kept constant). For each simulation there are five time-steps defined: long and short time-step of the Eulerian component (the short one used for sound-wave terms), the time-step used for integrating the condensational growth/evaporation equation, the time-step used for solving collisional growth using the Monte-Carlo scheme, and the time-step for integration of particle motion equations.

OAP-2DS mimicking analysis

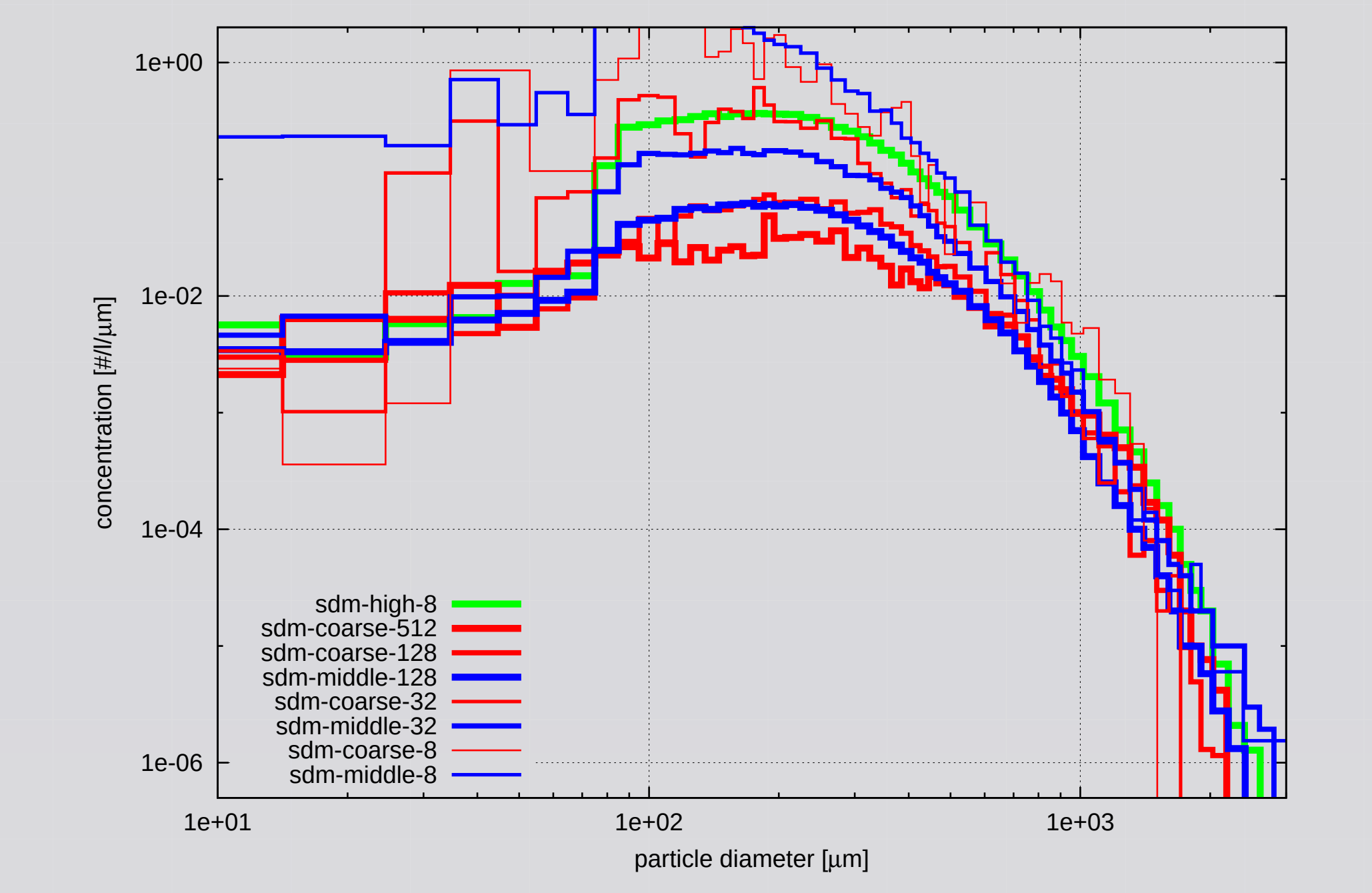

The figure is intended for comparison with Fig. 4 in Baker et al. (2009) based on measurement data obtained with the OAP-2DS instrument (Lawson et al., 2006) during RICO research flights. During RICO the OAP-2DS instrument was set to classify particles into 61 size bins spanning the 2.5 μm – 1.5 mm size range in radius. In the analysis of Baker et al. (2009) a mean size spectrum was derived from 237 spectra measured within rain-shafts below the cloud base at the altitude of about 183 metres (600 ft). In order to derive comparable quantities from the simulation results, the super-droplets in each grid cell were classified into size bins of the same layout as used by the OAP-2DS instrument, an altitude range of 183 ± 100 m was chosen, and only grid cells with rain water mixing ratio $q_r > 0.001$ g/kg were taken into account (q_r being derived from summation over super-droplets with radii greater than 40 μm).

outline

We present a series of Large Eddy Simulations (LES) employing the Super-Droplet Method (SDM) for representing aerosol, cloud and warm-rain microphysics (Shima, 2008; Shima et al., 2009). SDM is a particle-based and probabilistic Monte-Carlo type model.

The model does not differentiate between aerosol particles, cloud droplets, drizzle or rain drops. Each particle in the model (referred to as super-droplet) represents a multiplicity of real-world particles of the same size and of the same chemical composition.

The super-droplets are subject to (i) gravitational settling, (ii) condensational growth/evaporation and (iii) collisional growth.

salient features of the Super-Droplet approach

- diffusive error-free computational scheme for both condensational (moving-sectional type) and collisional growth (Monte-Carlo type)
- particle spectrum representation facilitating comparison with experimental data obtained with particle-counting instruments
- persistence of arbitrary number of scalar quantities assigned to a super-droplet (e.g. CCN physico-chemical properties)
- scalability in terms of sampling error (i.e. super-droplet density)
- parameterisation-free formulation of the key processes involved in cloud-aerosol interactions

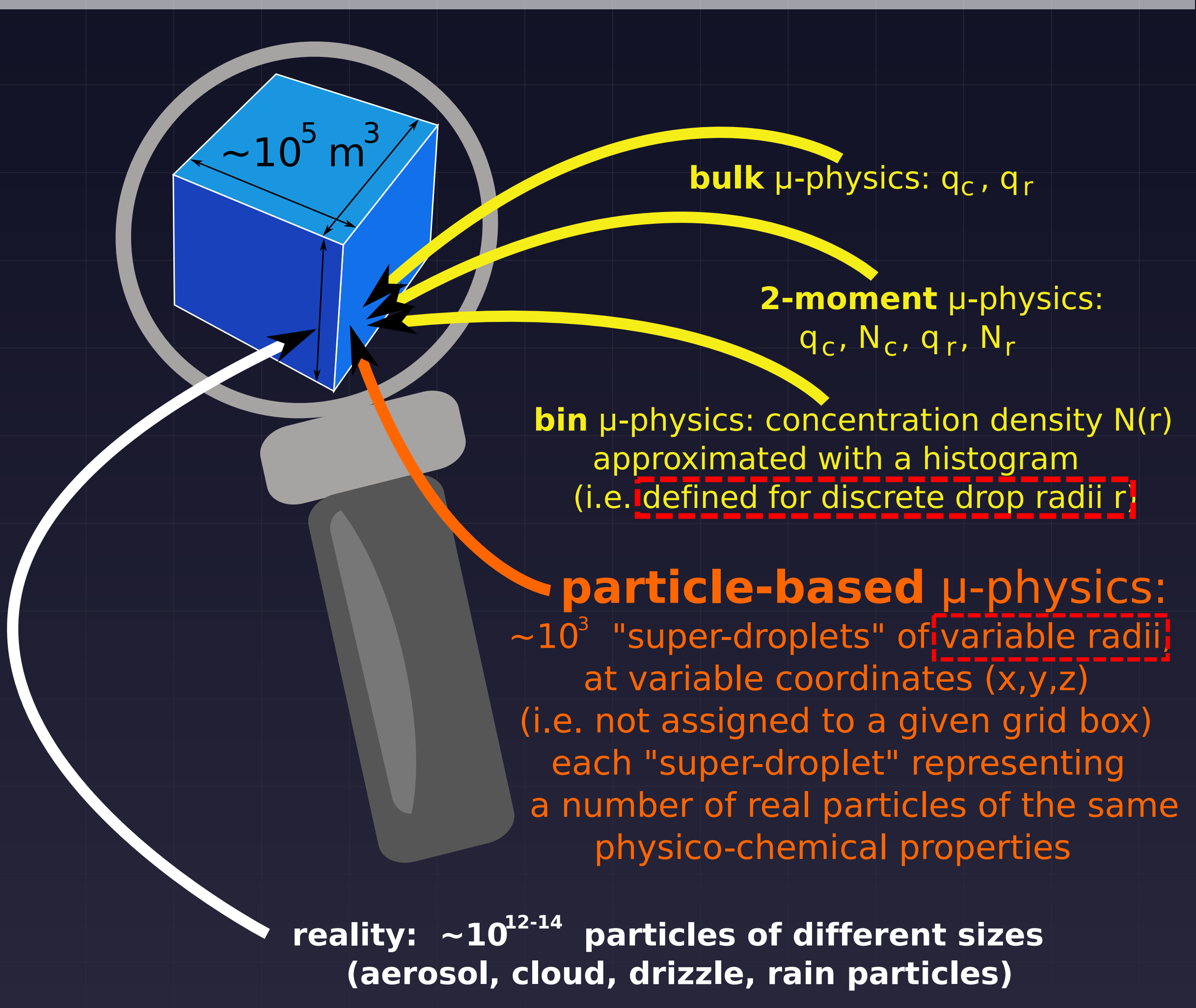

bulk µ-physics: q_c, q_r

2-moment µ-physics:
q_c, N_c, q_r, N_r

bin µ-physics: concentration density N(r)
approximated with a histogram
(i.e. defined for discrete drop radii r)

particle-based µ-physics:
~10^3 "super-droplets" of variable radii
at variable coordinates (x,y,z)
(i.e. not assigned to a given grid box)
each "super-droplet" representing
a number of real particles of the same
physico-chemical properties

reality: ~$10^{12\text{-}14}$ particles of different sizes
(aerosol, cloud, drizzle, rain particles)

Fast-FSSP-mimicking analysis...

... varying grid resolution

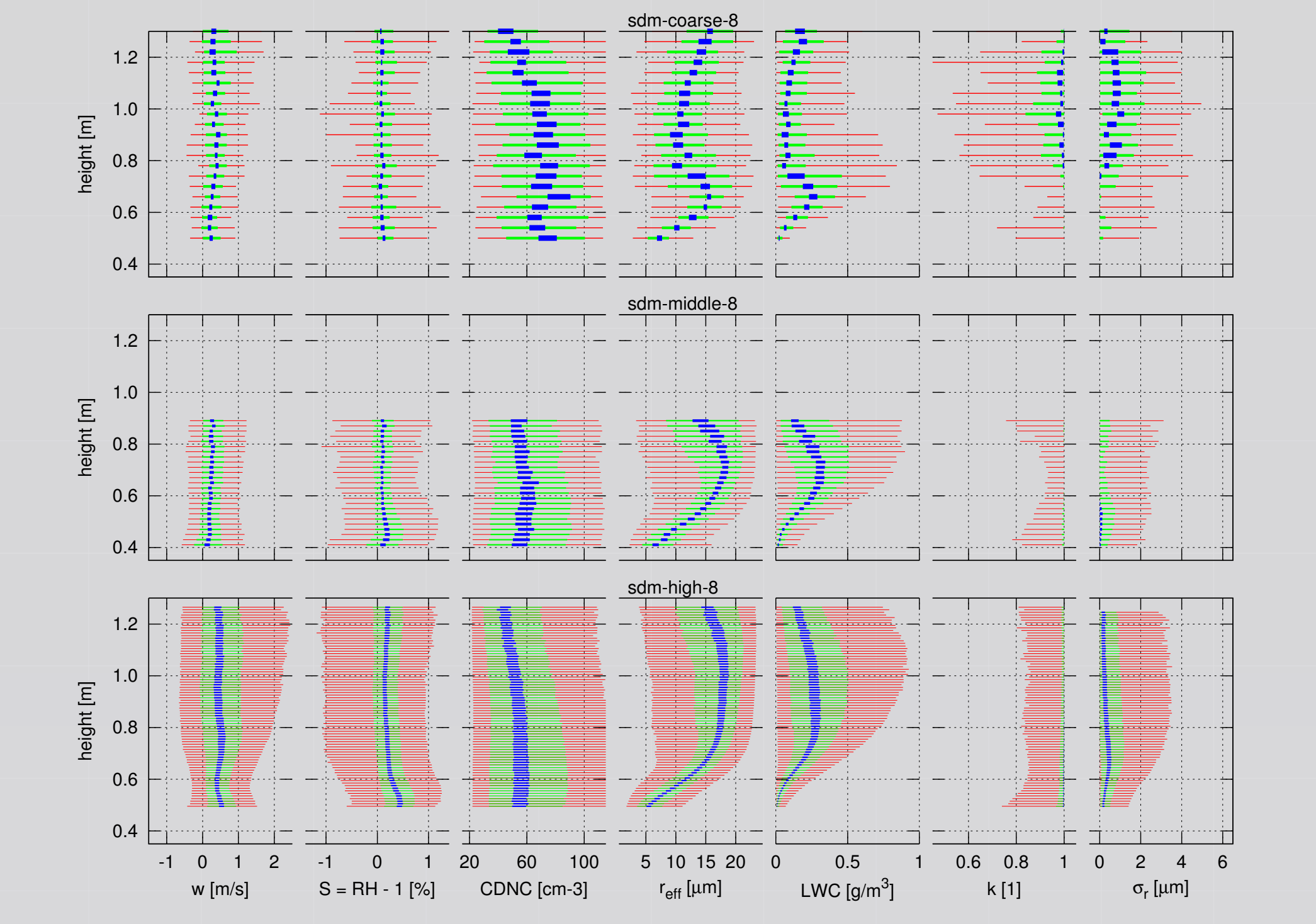

... varying Super-Droplet density

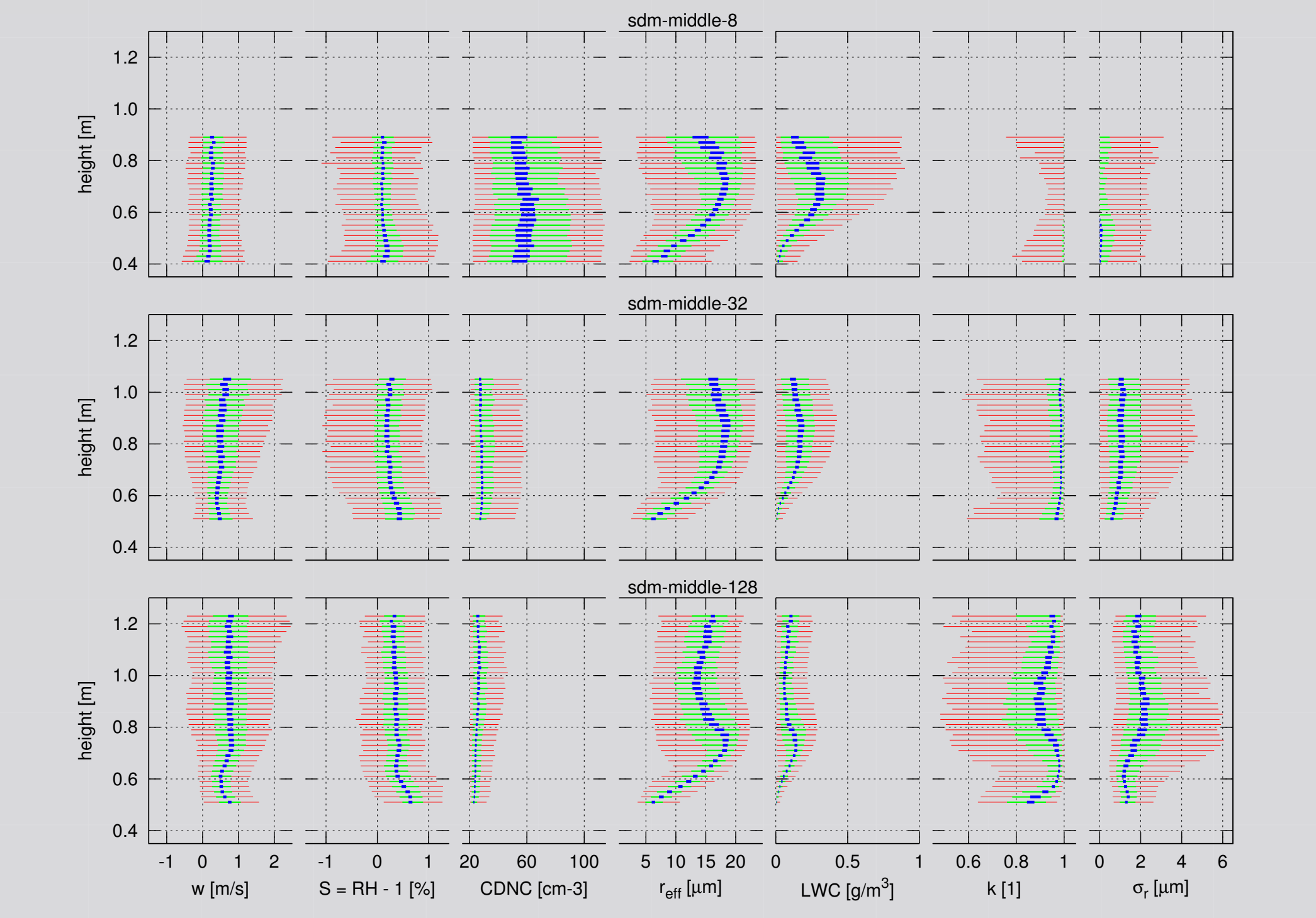

Figures present height-resolved statistics of the vertical velocity w, the supersaturation S, cloud droplet concentration CDNC, droplet effective radius r_{eff}, liquid water content LWC, the cubed ratio of mean volume radius to effective radius $k = \langle r^3 \rangle / r_{eff}$, and the standard deviation of cloud droplet radius σ_r. The plots are intended for comparison with the analysis presented in Arabas et al. (2009, Figs. 1 and 2) where the data from aircraft measurements during the RICO campaign using the Fast-FSSP optical cloud droplet spectrometer (Brenguier et al., 1998) were analysed. The herein analysis of SDM simulation data is constrained to in-cloud regions defined as the grid boxes having CDNC> 20 cm^{-3} where CDNC is derived by summing over the super-droplets representing particles of radius between 1 and 24 micrometres.

The choices of the CDNC threshold and the spectral range correspond to those characteristic of the Fast-FSSP probe. Plot construction method was chosen following the methodology of Arabas et al. (2009). For each level of the model grid and each plotted parameter a list of values matching the in-cloud criterion is constructed, sorted and linearly interpolated to find the 5th, 25th, 45th, 55th, 75th and 95th percentiles. The lists are constructed from the LES-grid values (w, S) or super-droplet statistics calculated for each grid cell (CDNC, r_{eff}, LWC, k and σ_r). The 5th – 95th percentile, the interquartile, and the 45th – 55th percentile ranges are plotted as a function of height using red, green and blue bars, respectively.

selected previously-published analyses of RICO in-situ cloud microphysics aircraft observations

Baker et al. 2009 (OAP-2DS probe)

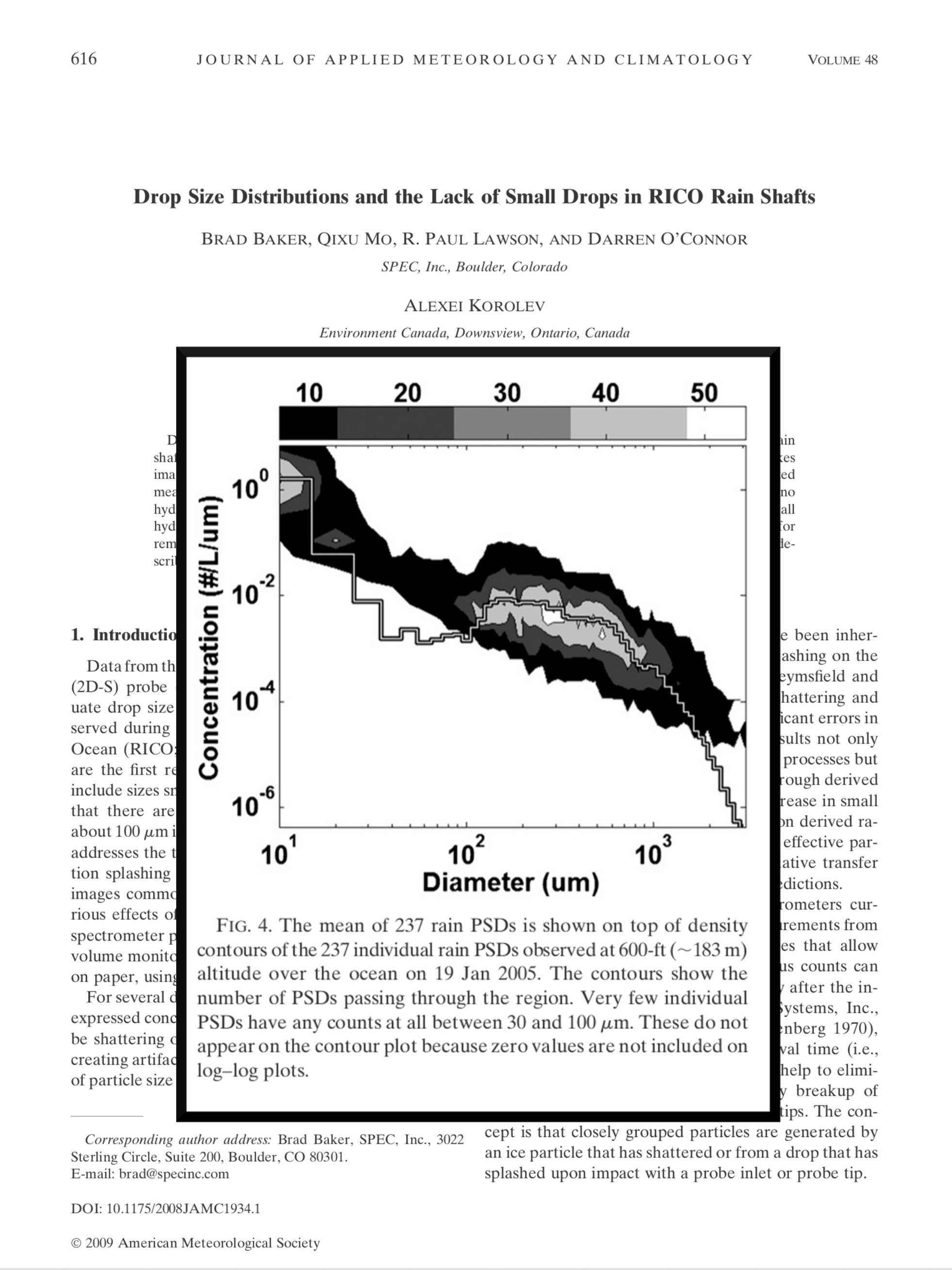
616 JOURNAL OF APPLIED METEOROLOGY AND CLIMATOLOGY VOLUME 48

Drop Size Distributions and the Lack of Small Drops in RICO Rain Shafts

BRAD BAKER, QIXU MO, R. PAUL LAWSON, AND DARREN O'CONNOR
SPEC, Inc., Boulder, Colorado

ALEXEI KOROLEV
Environment Canada, Downsview, Ontario, Canada

FIG. 4. The mean of 237 rain PSDs is shown on top of density contours of the 237 individual rain PSDs observed at 600-ft (~183 m) altitude over the ocean on 19 Jan 2005. The contours show the number of PSDs passing through the region. Very few individual PSDs have any counts at all between 30 and 100 μm. These do not appear on the contour plot because zero values are not included on log–log plots.

cept is that closely grouped particles are generated by an ice particle that has shattered or from a drop that has splashed upon impact with a probe inlet or probe tip.

Corresponding author address: Brad Baker, SPEC, Inc., 3022 Sterling Circle, Suite 200, Boulder, CO 80301.
E-mail: brad@specinc.com

DOI: 10.1175/2008JAMC1934.1

© 2009 American Meteorological Society

Brenguier et al. 2011 (Fast-FSSP probe)

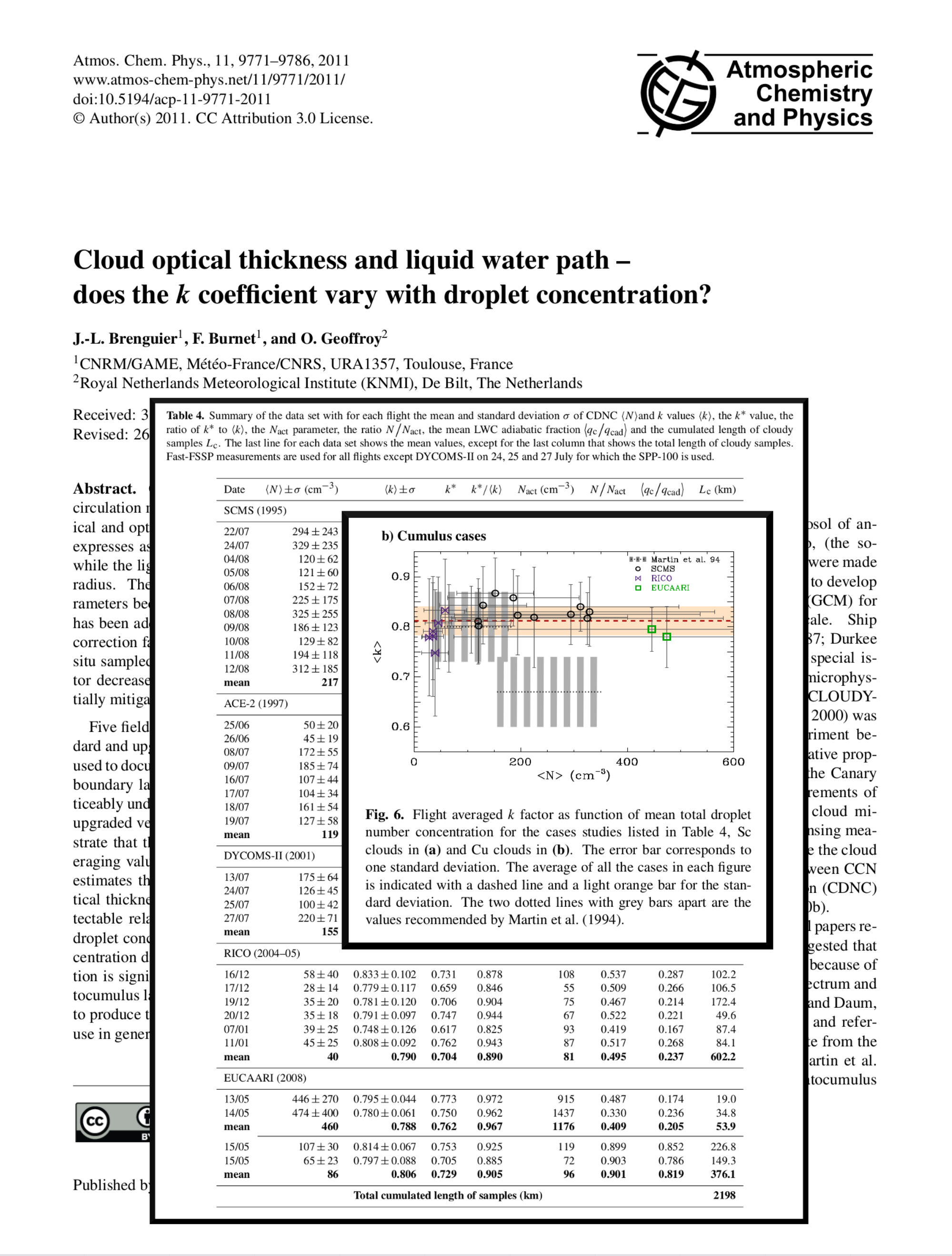
Atmos. Chem. Phys., 11, 9771–9786, 2011
www.atmos-chem-phys.net/11/9771/2011/
doi:10.5194/acp-11-9771-2011
© Author(s) 2011. CC Attribution 3.0 License.

Atmospheric Chemistry and Physics

Cloud optical thickness and liquid water path – does the *k* coefficient vary with droplet concentration?

J.-L. Brenguier[1], F. Burnet[1], and O. Geoffroy[2]

[1]CNRM/GAME, Météo-France/CNRS, URA1357, Toulouse, France
[2]Royal Netherlands Meteorological Institute (KNMI), De Bilt, The Netherlands

Table 4. Summary of the data set with for each flight the mean and standard deviation σ of CDNC ⟨N⟩and k values ⟨k⟩, the k* value, the ratio of k* to ⟨k⟩, the N_{act} parameter, the ratio N/N_{act}, the mean LWC adiabatic fraction $\langle q_c/q_{cad}\rangle$ and the cumulated length of cloudy samples L_c. The last line for each data set shows the mean values, except for the last column that shows the total length of cloudy samples. Fast-FSSP measurements are used for all flights except DYCOMS-II on 24, 25 and 27 July for which the SPP-100 is used.

Date	$\langle N\rangle\pm\sigma$ (cm^{-3})	$\langle k\rangle\pm\sigma$	k^*	$k^*/\langle k\rangle$	N_{act} (cm^{-3})	N/N_{act}	$\langle q_c/q_{cad}\rangle$	L_c (km)
SCMS (1995)								
22/07	294 ± 243							
24/07	329 ± 235							
04/08	120 ± 62							
05/08	121 ± 60							
06/08	152 ± 72							
07/08	225 ± 175							
08/08	325 ± 255							
09/08	186 ± 123							
10/08	129 ± 82							
11/08	194 ± 118							
12/08	312 ± 185							
mean	**217**							
ACE-2 (1997)								
25/06	50 ± 20							
26/06	45 ± 19							
08/07	172 ± 55							
09/07	185 ± 74							
16/07	107 ± 44							
17/07	104 ± 34							
18/07	161 ± 54							
19/07	127 ± 58							
mean	**119**							
DYCOMS-II (2001)								
13/07	175 ± 64							
24/07	126 ± 45							
25/07	100 ± 42							
27/07	220 ± 71							
mean	**155**							
RICO (2004–05)								
16/12	58 ± 40	0.833 ± 0.102	0.731	0.878	108	0.537	0.287	102.2
17/12	28 ± 14	0.779 ± 0.117	0.659	0.846	55	0.509	0.266	106.5
19/12	35 ± 20	0.781 ± 0.120	0.706	0.904	75	0.467	0.214	172.4
20/12	35 ± 18	0.791 ± 0.097	0.747	0.944	67	0.522	0.221	49.6
07/01	39 ± 25	0.748 ± 0.126	0.617	0.825	93	0.419	0.167	87.4
11/01	45 ± 25	0.808 ± 0.092	0.762	0.943	87	0.517	0.268	84.1
mean	**40**	**0.790**	**0.704**	**0.890**	**81**	**0.495**	**0.237**	**602.2**
EUCAARI (2008)								
13/05	446 ± 270	0.795 ± 0.044	0.773	0.972	915	0.487	0.174	19.0
14/05	474 ± 400	0.780 ± 0.061	0.750	0.962	1437	0.330	0.236	34.8
mean	**460**	**0.788**	**0.762**	**0.967**	**1176**	**0.409**	**0.205**	**53.9**
15/05	107 ± 30	0.814 ± 0.067	0.753	0.925	119	0.899	0.852	226.8
15/05	65 ± 23	0.797 ± 0.088	0.705	0.885	72	0.903	0.786	149.3
mean	**86**	**0.806**	**0.729**	**0.905**	**96**	**0.901**	**0.819**	**376.1**
Total cumulated length of samples (km)								**2198**

Fig. 6. Flight averaged k factor as function of mean total droplet number concentration for the cases studies listed in Table 4, Sc clouds in **(a)** and Cu clouds in **(b)**. The error bar corresponds to one standard deviation. The average of all the cases in each figure is indicated with a dashed line and a light orange bar for the standard deviation. The two dotted lines with grey bars apart are the values recommended by Martin et al. (1994).

Arabas et al. 2009 (Fast-FSSP probe)

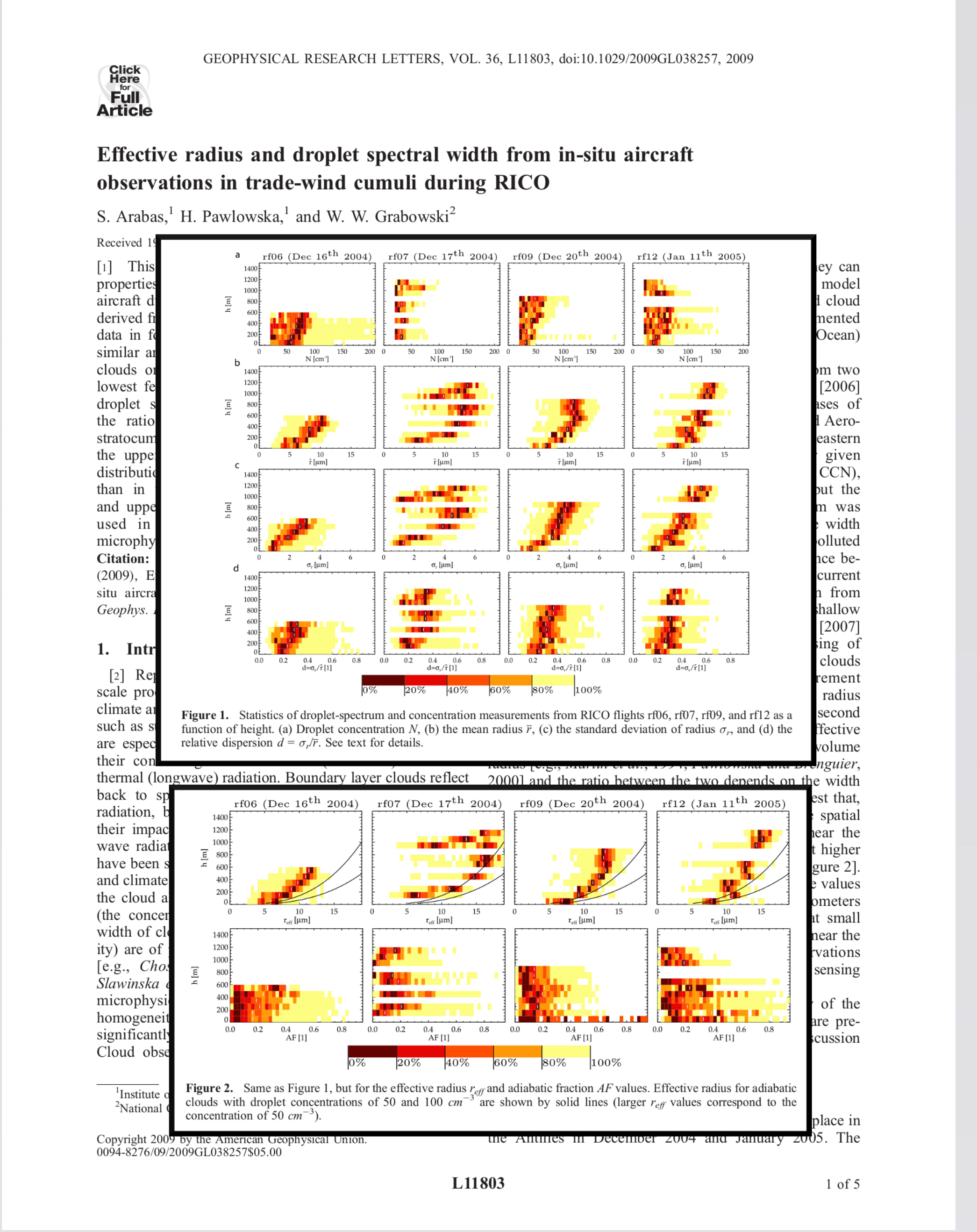
GEOPHYSICAL RESEARCH LETTERS, VOL. 36, L11803, doi:10.1029/2009GL038257, 2009

Click Here for Full Article

Effective radius and droplet spectral width from in-situ aircraft observations in trade-wind cumuli during RICO

S. Arabas,[1] H. Pawlowska,[1] and W. W. Grabowski[2]

Figure 1. Statistics of droplet-spectrum and concentration measurements from RICO flights rf06, rf07, rf09, and rf12 as a function of height. (a) Droplet concentration N, (b) the mean radius $\bar{r}$, (c) the standard deviation of radius σ_r, and (d) the relative dispersion $d = \sigma_r/\bar{r}$. See text for details.

Figure 2. Same as Figure 1, but for the effective radius r_{eff} and adiabatic fraction AF values. Effective radius for adiabatic clouds with droplet concentrations of 50 and 100 cm^{-3} are shown by solid lines (larger r_{eff} values correspond to the concentration of 50 cm^{-3}).

Thermal (longwave) radiation. Boundary layer clouds reflect

0094-8276/09/2009GL038257$05.00

L11803 1 of 5

Acknowledgements

All simulations were carried out on "The Earth Simulator 2" operated by the Japanese Agency for Marine-Earth Science and Technology (JAMSTEC) in Kanagawa, Japan. JAMSTEC supported a month-long research visit of SA to Japan, and provided computer time on the ES2. Thanks are due Hanna Pawlowska (University of Warsaw) and Kanya Kusano (JAMSTEC, Nagoya University) for their support throughout the project; and Kozo Nakamura (JAMSTEC) for his help with implementing the RICO set-up in CReSS.